QRS Detection Using Zero Crossing Counts

B.-U. KÖHLER, C. HENNIG, R. ORGLMEISTER
Biomedical Electronics Group, Department of Electrical Engineering, Berlin University of Technology, Berlin, Germany

Summary

There is a novel technique for the detection of QRS complexes in electrocardiographic signals that is based on a feature obtained by counting the number of zero crossings per segment. It is well-known that zero crossing methods are robust against noise and are particularly useful for finite precision arithmetic. The new detection method inherits this robustness and provides a high degree of detection performance even in cases of very noisy electrocardiographic signals. Furthermore, due to the simplicity of detecting and counting zero crossings, the proposed technique provides a computationally efficient solution to the QRS detection problem. The excellent performance of the algorithm is confirmed by a sensitivity of 99.70% (277 false negatives) and a positive predictivity of 99.57% (390 false positives) against the MIT-BIH arrhythmia database.

Key Words

Electrocardiography (ECG), ECG beat detection, QRS detection, zero crossings

Introduction

The importance of QRS detection results from the wide use of the timing information of this component, e.g., in heart rate variability analysis, ECG classification, and ECG compression. In most cases, the temporal location of the R-wave is taken as the location of the QRS complex. Missed or falsely detected beats are problematic in all of these applications and may lead to poor results. The literature [1,2] clearly indicates that the number of false detections may increase significantly in the presence of poor signal-to-noise ratios or pathological signals. Detection errors can be reduced by the application of computationally more expensive algorithms, for instance by the implementation of reverse search methods. However, particularly in the case of battery-driven devices, the computational complexity needs to be kept low. Hence, a tradeoff between computational complexity and detection performance needs to be found.

The detection of QRS complexes and R-waves in ECG signals has been studied for several decades. Most of the earliest algorithms are based on feature signals obtained from the derivatives of the ECG signal [3-9]. As long as no additional rules for the reduction of false detections are applied, these methods are characterized by low computational complexity and relatively poor detection results in the presence of problematic signals (e.g., containing baseline drift, noise and artifacts, as well as changes in the QRS morphology). For an overview of algorithms based on the first and second order derivative of the ECG, see [1].

Additionally, more sophisticated digital filters have been used as peak detectors for ECG signals, providing better feature signals for disturbed ECG signals [2,9-19]. Many standard signal processing methods have been applied to QRS and R-wave detection, such as methods from the field of linear and nonlinear filtering [20], wavelet transform [21-22], artificial neural networks [23-24], genetic algorithms [25], and linear prediction [26]. These algorithms [1,20-28] are generally much more complex compared to derivative-based methods and thus exhibit significantly better detection results.

In this paper, an algorithm is proposed that simultaneously meets the demands of a low computational load

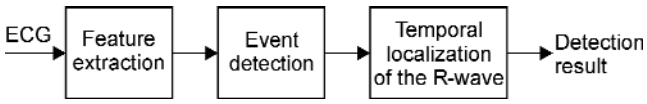

Figure 1. Stages of the algorithm.

and a high detection performance. The proposed method is based on a feature that is obtained by counting the number of zero crossings per segment. It is a feature signal that is largely independent of sudden changes in the amplitude level of the signal and is robust against noise and pathological signal morphologies. It is shown that this feature can be used for a computationally simple algorithm with a high detection performance.

Methods

Algorithm Overview

Figure 1 shows the block diagram of the algorithm. The algorithm consists of three stages: the extraction of the feature signal, the event detection, and the temporal localization of the R-wave.

Feature extraction: The frequency content of a QRS complex may extend up to 40 Hz and more, whereas P- and T-waves usually have frequency components of up to 10 Hz [20,30]. Due to these spectral characteristics of the ECG components, it is reasonable to filter the ECG signal at first in order to attenuate the mean, the P- and T-wave, and the high frequency noise. Because the filtered signal will be used for the temporal localization of the R-wave, it is important to use a band pass filter with a linear phase response. Otherwise, an accurate localization of the R-wave would be impossible. As depicted in Figure 2b, the band pass filtered signal oscillates around zero. During the QRS complex it has a high amplitude; otherwise its amplitude is low. Then, adding a low-power, high-frequency sequence to the band bass filtered signal as shown in Figure 2c leads to a signal that has many zero crossings during non-QRS segments and only a small number of zero crossings during the QRS complex. The high frequency sequence may be computed as

$$b(n) = (-1)^n \cdot K(n) \qquad (1)$$

where n denotes the time index and $K(n)$ is a time-varying amplitude. Counting the number of zero crossings per segment with a moving window leads to the feature signal depicted in Figure 2d. Characteristically the feature signal assumes low values during a QRS complex and high values otherwise. The maximum value of the feature signal is given by the length N of the moving window. The feature generation is based on the Dominant Frequency Principle known from the literature [31]. The number of zero crossings per segment is an equivalent representation of the frequency of the dominant component of a signal segment. It can be considered as roughly proportional to the dominant frequency. Accordingly, for a low-frequency component one can expect fewer zero crossings per segment than for a high-frequency component. After the addition of the high-frequency sequence $b(n)$, the signal is dominated by a low-frequency oscillation during the QRS complex and dominated by the high-frequency sequence otherwise. Hence, the number of zero crossings must be low during the QRS complex and high at all other times.

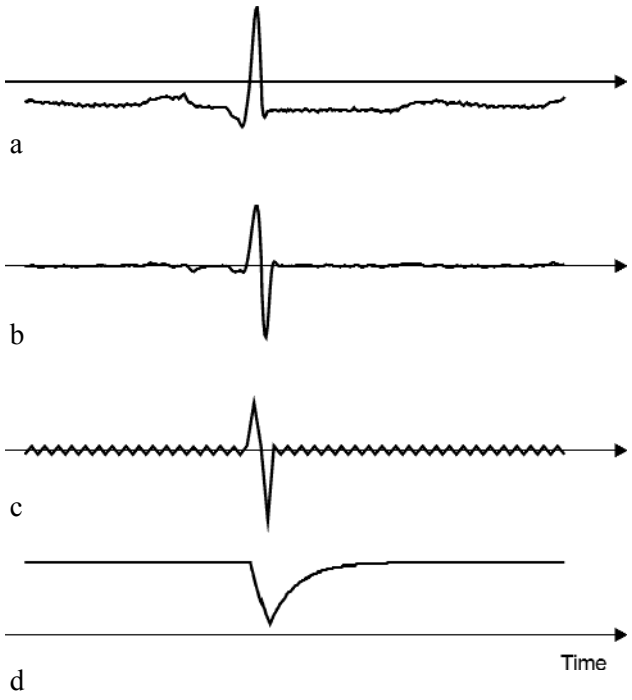

Figure 2. Qualitative time course of the signals in the feature extraction stage. Panel a) original ECG signal, panel b) band pass filtered ECG signal, panel c) signal after adding the high-frequency sequence, panel d) zero crossing count (exponential window).

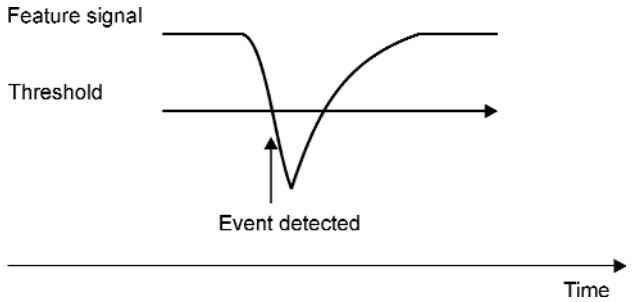

Figure 3. Event detection.

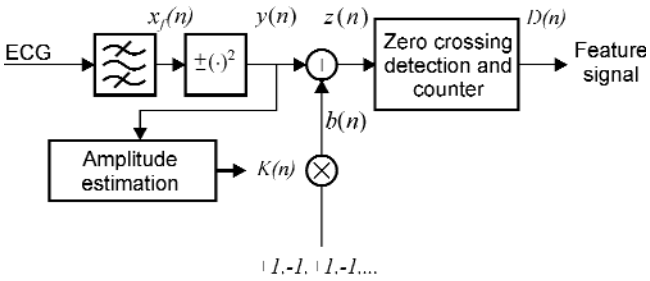

Figure 4. Block diagram of the feature extraction.

Event Detection: An event begins when the feature signal (number of zero crossings per segment) falls below a signal-adaptive threshold as shown in Figure 3. The events ends when the signal rises above the threshold. Both the beginning and the end of the event are the boundaries of the search interval for the temporal localization of the R-wave. If adjacent events are temporally very close (multiple events), they will be combined into one single event. The beginning of the combined event is the beginning of the first event, and the end of the combined event is the end of the last event.

Temporal localization of the R-wave: The detection of the QRS complex is completed by the determination of the temporal location of the R-wave. If only one ECG channel is used for the detection of the R-wave, the electrical position of the heart needs to be taken into consideration. For that purpose the temporal location is determined by a combined maximum/minimum search. A simple decision logic decides whether to use the maximum or the minimum position of the search interval as the temporal location of the R-wave.

Detailed Description of the Feature Extraction

Block diagram of the feature extraction: The block diagram of the QRS detection algorithm is shown in Figure 4. It consists of a band pass filter, a non-linear transform, the amplitude estimation and addition of the high-frequency sequence, the zero crossing detection, and the zero crossing counter. The input signal is the original ECG, and the output is the feature signal.

Linear and nonlinear filtering: As in most conventional algorithms, band pass filtering is performed as a preprocessing method in order to increase the signal to noise ratio, i.e., to attenuate the mean, the P- and the T-wave, as well as some high-frequency noise. In our implementation a 27 tap linear phase FIR filter is used. The cut-off frequencies are 18 Hz and 35 Hz. In some cases, simpler filters may be sufficient. In case of insignificant high-frequency components, the low pass part of the band pass can be omitted. A further increase in the signal quality is achieved by a nonlinear transform of the signal

$$y(n) = sign(x_f(n)) \cdot x_f^2(n) \tag{2}$$

where $x_f\ (n)$ denotes the band pass filtered ECG and $y(n)$ denotes the non-linearly transformed signal.
The signal $y(n)$ will be used later for the determination of the temporal location of the R-wave.

Amplitude estimation and addition of a high-frequency sequence: Due to the application of the band pass filter within the signal $y(n)$, high-frequency oscillations are strongly attenuated. Hence, it is necessary to add a high-frequency sequence

$$b(n) = (-1)^n \cdot K(n) \tag{3}$$

to the signal, i.e.,

$$z(n) = y(n) + b(n) \tag{4}$$

in order to increase the number of zero crossings during non-QRS segments. In the ideal case, the feature signal $D(n)$ assumes the value $D(n) = N$ during non-QRS segments and $D(n) < N$ during the QRS complex as depicted in Figure 2. However, if the amplitude $K(n)$ of the high-frequency sequence $b(n)$ is too large, the number of zero crossings is always N. If $K(n)$ is too small, the feature signal is noisy, and the difference between the number of zero crossings during the QRS segments and non-QRS segments is not significant

enough for a good classification. Hence, the amplitude *K(n)* of the sequence must be properly determined. In our implementation, *K(n)* is determined from the magnitude of the signal *y(n)*

$$K(n) = \lambda_K K(n-1) + (1-\lambda_K)\left|y(n)\right| \cdot c \qquad (5)$$

where $\lambda_K \in (0;1)$ is a forgetting factor, and the design parameter c denotes a constant gain, e.g., *c = 4*.

Detection and Counting of Zero Crossings: There are several methods for the detection of zero crossings; for an overview see [31]. In our implementation we use

$$d(n) = \left|\frac{sign[z(n)] - sign[z(n-1)]}{2}\right| \qquad (6)$$

The number of zero crossings per segment is usually computed by

$$D(n) = \sum_{i=0}^{N-1} d(n-i) \qquad (7)$$

The operation in Equation 7 is a low pass filtering operation. Although it can be implemented in a computationally efficient way by some delays and one feedback connection, this type of filter is not used. Instead of the filter in Equation 7, a first order autoregressive low pass filter is implemented, i.e.,

$$D(n) = \lambda_D D(n-1) + (1-\lambda_D)d(n) \qquad (8)$$

where $\lambda_D \in (0;1)$ is a forgetting factor. Similarly to the filter in Equation 7, the filter in Equation 8 can also be implemented very efficiently. Furthermore, with respect to a processor or direct hardware implementation, the latter filter has the advantage of being more easily adjustable and less memory-consuming.

Detailed Description of Event Detection

Event detection is accomplished using an adaptive threshold θ. It is computed from the feature signal as

$$\Theta(n) = \lambda_\Theta \Theta(n-1) + (1-\lambda_\Theta)D(n) \qquad (9)$$

where $\lambda_\Theta \in (0;1)$ represents a forgetting factor. For the detection of an event, the threshold $\theta(n)$ is compared to the feature signal *D(n)*. When *D(n)* falls below the threshold an event is detected. This simple detection logic is suitable for a smooth feature signal. However, in some cases the feature signal has more than one peak for one QRS complex, as shown in Figure 5. In order to prevent the algorithm from detecting multiple

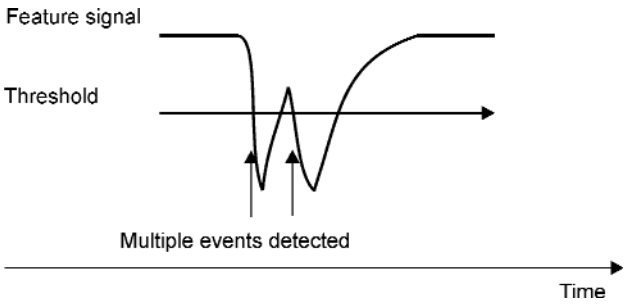

Figure 5. Detection of multiple events.

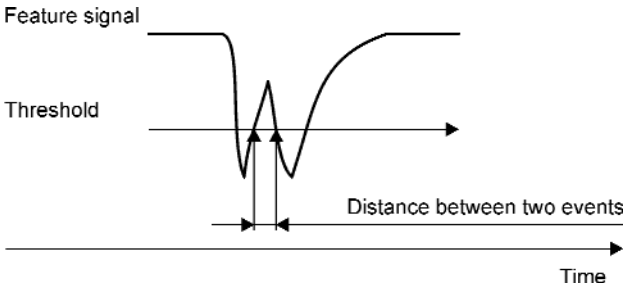

Figure 6. Distance between two events.

events, a refinement is necessary. For that reason the distance between events is considered. The distance between two events is defined, according to the drawing in Figure 6, as the time between the end of one event and the beginning of the next. If the distance between two detected events is too short, both events are combined into one single event. This method can be implemented very easily in a serial processing mode by using a timer that provides a time-out after some time past the end of the last event. The end of the event is only valid if the next event starts after the time-out. Otherwise, both events are combined into one single event. A valid end triggers the search for the temporal location of the R-wave.

Temporal Localization of the R-wave

The beginning and the end, i.e., the temporal location of the event, provide the bounds for the search interval that is used for the temporal localization of the R-wave. The electrical position of the heart has a great impact on the amplitude and the sign of the R-wave. For this reason, a combined maximum/minimum search in the signal *y(n)* is carried out. If the magnitude of the minimum is much larger than the magnitude of

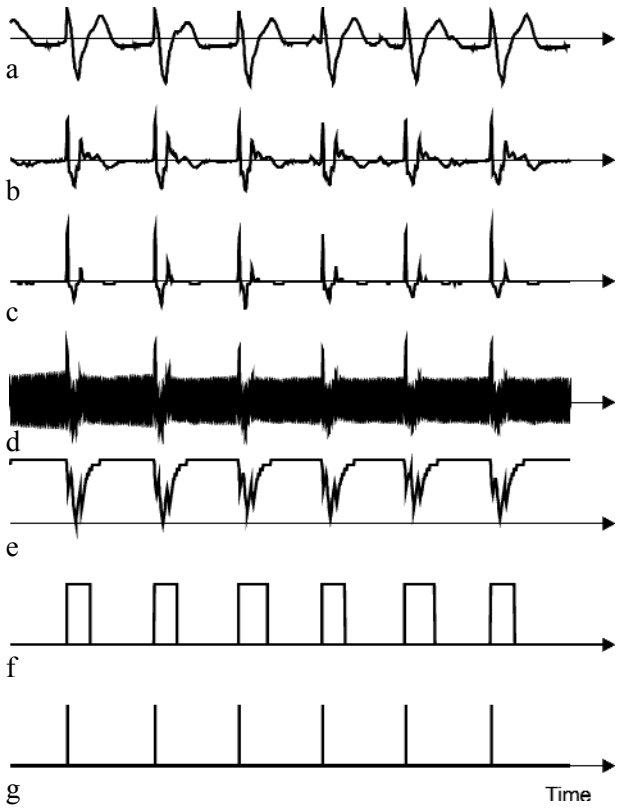

Figure 7. Segment from record 107 of the MIT-BIH arrhythmia database [32]. Panel a) original ECG signal, panel b) ECG signal after the band pass filter xf (n), panel c) ECG signal after the non-linearity y(n), panel d) signal after the addition of the high-frequency sequence z(n), panel e) feature signal D(n), panel f) event signal (low: no event, high: during event), panel g) detected beats after the temporal localization of the R-wave.

the maximum, the temporal location of the minimum is taken as the time of the R-wave. Otherwise, the maximum position determines the location of the R-wave. For the actual position of the R-wave, the group delay of the band pass filter needs to be taken into consideration.

Example

Figure 7 depicts several signals from the different stages of the algorithm. The signal segment is taken from record 107 of the MIT/BIH Arrhythmia Database [32]. It is clear that the band pass filter is far from perfect. A great increase in the signal to noise ratio is achieved by the non-linearity. The feature signal shows the typical exponentially shaped time course, which is due to the application of the first order autoregressive averaging filter. As described in the previous subsection, the feature signal has more than one minimum per QRS complex in most cases. However, due to combining close multiple events into one single event, multiple detections are mostly avoided.

Results

The algorithm was validated against the MIT-BIH arrhythmia database. Each record of the database consists of two channels. Only the first channel was used for evaluating the performance of the algorithm. The first 5 minutes of a record are generally considered as a training set [32] and hence left unconsidered within the statistics. As performance measures, the indices from [33], [20] were used, i.e.,

$$Se = \frac{TP}{TP + FN} \quad sensitivity \tag{10}$$

$$+P = \frac{TP}{TP + FP} \quad positive\ predictivity \tag{11}$$

where TP denotes the number of true positives, FN is the number of false negatives, and FP is the number of false positives. A beat is considered as correctly detected within a window of ± 75 ms around the true temporal beat location. The algorithm was implemented using the Visual C++ programming language. On a 450 MHz Pentium III personal computer the algorithm required about 7 s to process a 0.5-hour record of the MIT-BIH Arrhythmia Database. Table I shows the results of the algorithm. The sensitivity of the algorithm is 99.70% (277 FNs) and its positive predictivity 99.57% (390 FPs). The largest number of false positive detections were in record 207. This record is particularly difficult for the algorithm. For many very noisy records, for example record 108, the algorithm achieves not perfect but fairly good results. In some records, the last R-wave is located very close to the end of the record, e.g., in record 100. Due to the delay of the algorithm those beats are not detected.

Discussion

The algorithm has only a few parameters, e.g., the band pass filter, the forgetting factors λ_K, λ_D, and λ_Θ, the constant gain c, the timeout period in the event

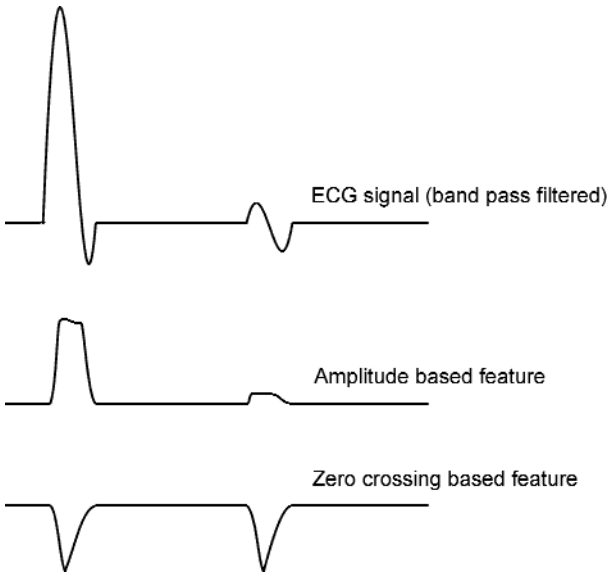

Figure 8. Comparison between amplitude based features and the zero crossing based feature: the zero crossing based feature is robust against amplitude level variations of the ECG signal.

detection stage, and the threshold of the sign decision within the R-wave localization. If physiologically reasonable forgetting factors and timeout periods are chosen, the algorithm works reliably, also in cases of minor parameter maladjustments. Due to the non-linear type of the algorithm, the impact of the different parameters on the performance is not independent from each other. However, from our experience with this algorithm, the impact of these interdependencies does not lead to real tuning problems. The band pass filter has a great impact on the performance of the algorithm. It is most important that this filter removes the P-wave and the T-wave. Hence, this filter needs to be chosen carefully. If only one of these components remains within the signal, the algorithm will fail.

The number of zero crossings per segment is a good feature for event detection. One major reason is its robustness against amplitude level variations of the ECG. QRS detection methods that are comparable with respect to the computational load often use first

Table 1. Performance of the zero crossing based QRS detection algorithm on MIT/BIH database [32].

Tape no.	Channel	TP	FN	FP	Se (%)	+P (%)
100	MLII	1901	1	0	99.95	100.00
101	MLII	1521	2	5	99.87	99.67
102	V5	1808	13	13	99.29	99.29
103	MLII	1729	0	0	100.00	100.00
104	V5	1841	16	17	99.14	99.09
105	MLII	2144	11	28	99.49	98.71
106	MLII	1696	0	5	100.00	99.71
107	MLII	1783	1	0	99.94	100.00
108	MLII	1454	26	32	98.24	97.85
109	MLII	2094	5	1	99.76	99.95
111	MLII	1774	2	4	99.89	99.78
112	MLII	2111	0	4	100.00	99.81
113	MLII	1505	1	0	99.93	100.00
114	V5	1604	0	5	100.00	99.69
115	MLII	1636	1	0	99.94	100.00
116	MLII	1995	22	3	98.91	99.85
117	MLII	1284	0	3	100.00	99.77
118	MLII	1916	0	3	100.00	99.84
119	MLII	1661	0	0	100.00	100.00
121	MLII	1558	2	4	99.87	99.74
122	MLII	2054	0	0	100.00	100.00
123	MLII	1269	0	2	100.00	99.84
24	MLII	1365	2	3	99.85	99.78
200	MLII	2166	2	12	99.91	99.45
201	MLII	1519	2	1	99.87	99.93
202	MLII	1868	3	3	99.84	99.84
203	MLII	2424	57	25	97.70	98.98
205	MLII	2197	4	0	99.82	100.00
207	MLII	1585	7	95	99.56	94.35
208	MLII	2413	24	7	99.02	99.71
209	MLII	2513	5	6	99.80	99.76
210	MLII	2198	6	2	99.73	99.91
212	MLII	2285	0	5	100.00	99.78
213	MLII	2680	20	17	99.26	99.37
214	MLII	1877	1	4	99.95	99.79
215	MLII	2793	2	0	99.93	100.00
217	MLII	1843	2	2	99.89	99.89
219	MLII	1773	0	0	100.00	100.00
220	MLII	1694	0	0	100.00	100.00
221	MLII	1998	22	19	98.91	99.06
222	MLII	2115	1	2	99.95	99.91
223	MLII	2199	0	1	100.00	99.95
228	MLII	1700	3	43	99.82	97.53
230	MLII	1859	0	2	100.00	99.89
231	MLII	1278	0	0	100.00	100.00
232	MLII	1485	0	12	100.00	99.20
233	MLII	2553	8	0	99.69	100.00
234	MLII	2288	3	0	99.87	100.00
Total:		91006	277	390	99.70	99.57

and second derivatives for the formation of the feature. Although the number of zero crossings per segment is not independent of the steepness, i.e., the derivative of the signal, the number of zero crossings contains additional information that is advantageous for QRS detection: For derivative-based feature signals, variations in the amplitude level or the morphology of the R-peak result in changes of derivative-based feature signals. In contrast to this, the number of zero crossings does not change with the amplitude variations in problematic sections of the ECG signal (Figure 8). This characteristic leads to a significant improvement of the detection performance on the level of computational expensive algorithms (e.g., [20] and [21]). The results in Table I show that for the formation of a feature signal, the number of zero crossings is superior to the derivative. Of course, the sensitivity depends on the amplitude *K(n)* of the high-frequency sequence *b(n)*. However, this amplitude is easily controllable by the algorithm. The algorithm inherits its robustness against noise from the general robustness of zero crossing signal processing methods against noise. The combination of temporarily close events into one single event replaces the usual refractory period. Furthermore, it prevents the execution of several R-wave searches for only one QRS complex and hence increases the efficiency of the algorithm.

The computational load is low. The computationally most consuming stages are the band pass filter and the maximum/minimum search for the temporal localization of the R-wave. Downsampling, as carried out in other algorithms, e.g. [20], is generally possible. However, because the algorithm utilizes the morphology of the signal, i.e., the oscillation of the QRS complex, it does not seem to be reasonable to use a sampling rate below 150 Hz.

Conclusion

A QRS detection algorithm based on zero crossings is presented. To our knowledge, it is the first time that this signal processing method has been applied to QRS detection. It has been shown that the number of zero crossings is a valuable feature that can be used for QRS detection purposes. The performance of the algorithm is comparable to other algorithms reported in the literature. Due to this simple principle, QRS detection can be realized at low computational costs.

References

[1] Friesen GM, Jannett TC, Jadallah MA, et al. A comparison of the noise sensitivity of nine QRS detection algorithms. IEEE Trans Biomed Eng. 1990; 37: 85-98.

[2] Pan J, Tompkins W. A real-time QRS detection algorithm. IEEE Trans Biomed Eng. 1985; 32: 230-236.

[3] Ahlstrom W, Tompkins W. Automated high-speed analysis of holter tapes with microcomputers. IEEE Trans Biomed Eng. 1983; 3: 651-657.

[4] Balda R. Trends in Computer-Processed Electrocardiograms. Amsterdam: North-Holland Publishing Company. 1977: 197-205.

[5] Fraden J, Neumann M. QRS wave detection. Med Biol Eng Comp. 1980; 18: 125-132.

[6] Gustafson D. Automated VCG Interpretation Studies Using Signal Analysis Techniques. Draper Report No. R-1044. Cambridge, MA: Charles Stark Draper Laboratory. 1977.

[7] Holsinger W, Kempner K, Miller M. A QRS pre-processor based on digital differentiation. IEEE Trans Biomed Eng. 1971; 18: 121-217.

[8] Morizet-Mahoudeaux P, Moreau C, Moreau D, et al. Simple microprocessor-based system for online ECG arrhythmia analysis. Med Biol Eng Comp. 1981; 19: 497-501.

[9] Okada M. A digital filter for the QRS complex detection. IEEE Trans Biomed Eng. 1979; 26: 700-703.

[10] Börjesson P, Pahlm O, Sörnmo L, et al. Adaptive QRS detection based on maximum a posteriori estimation. IEEE Trans Biomed Eng.1982; 29: 341-351.

[11] Engelse WAH, Zeelenberg C. A single scan algorithm for QRS-detection and feature extraction. Proceedings of the IEEE (Institute of Electrical and Electronics Engineers) Conference on Computers in Cardiology. 1979 Sep; Long Beach, USA. Los Alamitos: IEEE Computer Society Press. 1979: 37-42.

[12] Hamilton PS, Tompkins WJ. Quantitative investigation of QRS detection rules using the MIT/BIH arrhythmiac database. IEEE Trans Biomed Eng. 1986; 33: 1157-1165.

[13] Keselbrener L, Keselbrener M, Akselrod S. Nonlinear high pass filter for R-wave detection in ECG signal. Med Eng Phys. 1997; 19: 481- 484.

[14] Leski J, Tkacz E. A new parallel concept for QRS complex detector. Proceedings of the 14th Annual International Conference of the IEEE Engineering in Medicine & Biology Society (IEEE-EMBS). 1992 Oct 29 – Nov 1; Paris, France. Los Alamitos: IEEE Computer Society Press. 1992: 555-556.

[15] Ligtenberg A, Kunt M. A robust-digital QRS detection algorithm for arrhythmia monitoring. Comput Biomed Res. 1983; 16: 273-286.

[16] Nygards M-E, Hulting J. An automated system for ECG monitoring. Comput Biomed Res.1979;12: 181-202.

[17] Sörnmo L, Pahlm O, Nygaards ME. Adaptive QRS detection in ambulatory ECG monitoring: A study of performance. Proceedings of the IEEE (Institute of Electrical and Electronics Engineers) Conference on Computers in Cardiology. 1982; Seattle, USA. Los Alamitos: IEEE Computer Society Press. 1982: 201-204.

[18] Suppappola S, Sun Y. Nonlinear transforms of ECG signals for digital QRS detection: A quantitative analysis. IEEE Trans Biomed Eng. 1994; 41: 397-400.

[19] Yu B, Liu S, Lee M, et al. A nonlinear digital filter for cardiac QRS complex detection. J Clin Eng. 1985; 10: 193-201.

[20] Afonso VX, Tompkins WJ, Nguyen TQ, et al. ECG beat detection using filter banks. IEEE Trans Biomed Eng. 1999; 46: 192-202.

[21] Li C, Zheng C, Tai C. Detection of ECG characteristic points using wavelet transforms. IEEE Trans Biomed Eng. 1995; 42: 21-28.

[22] Kadambe S, Murray R, Boudreaux-Bartels GF. Wavelet transform-based QRS complex detector. IEEE Trans Biomed Eng. 1999; 46: 838-848.

[23] Xue Q, Hu YH, Tompkins WJ. Neural-network-based adaptive matched filtering for QRS detection. IEEE Trans Biomed Eng. 1992; 39: 317-329.

[24] Hu YH, Tompkins WJ, Urrusti JL, et al. Applications of artificial neural networks for ECG signal detection and classification. J Electrocardiol.1993; 26: 66-73.

[25] Poli R, Cagnoni S, Valli G. Genetic design of optimum linear and nonlinear QRS detectors. IEEE Trans Biomed Eng.1995; 42: 1137-1141.

[26] Lin KP, Chang WH. QRS feature extraction using linear prediction. IEEE Trans Biomed Eng. 1989; 36: 1050-1055.

[27] Ruha A, Sallinen S, Nissila S. A eral-time microprocessor QRS detector system with a 1-ms timing accuracy for the measurement of ambulatory HRV. IEEE Trans Biomed Eng. 1997; 44: 159-167.

[28] Laguna P, Jane R, Olmos S, et al. Adaptive estimation of QRS complex wave features of ECG signal by the Hermite model. Med Biol Eng Comp. 1996; 34: 58-68.

[29] Trahanias PE. An approach to QRS complex detection using mathematical morphology. IEEE Trans Biomed Eng. 1993; 40: 201-205.

[30] Tompkins WJ (editor). Biomedical Digital Signal Processing. Englewood Cliffs, NJ: Prentice Hall. 1993.

[31] B. Kedem. Time Series Analysis by Higher Order Crossings. Piscataway, NJ: IEEE Press. 1994.

[32] MIT-BIH Arrythmia Database, 2nd edition. Cambridge, MA: Massachusetts Institute of Technology, Biomedical Engineering Center. 1992. Available from: URL: http://www.physionet.org/physiobank/database/html/mitdbdir/mitdbdir.htm

[33] Recommended Practice for Testing and Reporting Performance Results of Ventricular Arrhythmia Detection Algorithms (AAMI ECAR-1987). Arlington, VA: Association for the Advancement of Medical Instrumentation (AAMI). 1987.

Contact
Dr. Bert-Uwe Köhler
Biomedical Electronics Group
Department of Electrical Engineering
Berlin University of Technology
Einsteinufer 17/EN3
D-10587 Berlin
Germany
Fax: + 49 (0)30 314 22120
E-mail: koehler@tubife1.ee.tu-berlin.de